THE JOURNAL OF BIOLOGICAL CHEMISTRY VOL. 289, NO. 28, pp. 19585–19598, July 11, 2014

Co-Activation of Nuclear Factor-κB and Myocardin/Serum Response Factor Conveys the Hypertrophy Signal of High Insulin Levels in Cardiac Myoblasts*

Received for publication, December 7, 2013, and in revised form, May 11, 2014 Published, JBC Papers in Press, May 22, 2014, DOI 10.1074/jbc.M113.540559

Rosalinda Madonna[‡§], Yong-Jian Geng[‡], Roberto Bolli[¶], Gregg Rokosh[¶], Peter Ferdinandy[‖], Cam Patterson[**], and Raffaele De Caterina[§1]

*From the [‡]Texas Heart Institute and University of Texas Medical School in Houston, Houston, Texas 77030, the [§]Institute of Cardiology, and Center of Excellence on Aging, "G. d'Annunzio" University, 66100 Chieti, Italy, the [¶]Institute of Molecular Cardiology, University of Louisville, Louisville, Kentucky 40202, the [‖]Department of Pharmacology and Pharmacotherapy, Semmelweis University, H-1085 Budapest, Hungary, and the **Center for Molecular Cardiology, The University of Texas Medical Branch at Galveston, Galveston, Texas 77555*

Background: Mechanisms of cardiac hypertrophy in states of insulin resistance/high insulin remain poorly understood.
Results: In response to high insulin, myocardin/SRF expression in cardiac myoblasts is related to the development of cardiac myoblast hypertrophy.
Conclusion: Myocardin acts, with Nuclear Factor-κB, as a nuclear effector of insulin, promoting cardiac hypertrophy.
Significance: Understanding these mechanisms may help designing strategies to prevent diabetic cardiomyopathy.

Hyperinsulinemia contributes to cardiac hypertrophy and heart failure in patients with the metabolic syndrome and type 2 diabetes. Here, high circulating levels of tumor necrosis factor (TNF)-α may synergize with insulin in signaling inflammation and cardiac hypertrophy. We tested whether high insulin affects activation of TNF-α-induced NF-κB and myocardin/serum response factor (SRF) to convey hypertrophy signaling in cardiac myoblasts. In canine cardiac myoblasts, treatment with high insulin (10^{-8} to 10^{-7} M) for 0–24 h increased insulin receptor substrate (IRS)-1 phosphorylation at Ser-307, decreased protein levels of chaperone-associated ubiquitin (Ub) E3 ligase C terminus of heat shock protein 70-interacting protein (CHIP), increased SRF activity, as well as β-myosin heavy chain (MHC) and myocardin expressions. Here siRNAs to myocardin or NF-κB, as well as CHIP overexpression prevented (while siRNA-mediated CHIP disruption potentiated) high insulin-induced SR element (SRE) activation and β-MHC expression. Insulin markedly potentiated TNF-α-induced NF-κB activation. Compared with insulin alone, insulin+TNF-α increased SRF/SRE binding and β-MHC expression, which was reversed by the NF-κB inhibitor pyrrolidine dithiocarbamate (PDTC) and by NF-κB silencing. In the hearts of db/db diabetic mice, in which Akt phosphorylation was decreased, p38MAPK, Akt1, and IRS-1 phosphorylation at Ser-307 were increased, together with myocardin expression as well as SRE and NF-κB activities. In response to high insulin, cardiac myoblasts increase the expression or the promyogenic transcription factors myocardin/SRF in a CHIP-dependent manner. Insulin potentiates TNF-α in inducing NF-κB and SRF/SRE activities. In hyperinsulinemic states, myocardin may act as a nuclear effector of insulin, promoting cardiac hypertrophy.

Myocardial hypertrophy, resulting from increased hemodynamic load or hormonal stimuli, tends to progress to cardiac dysfunction and heart failure (1). *In vitro* (2) and *in vivo* evidence from animal (3–5) and clinical studies (6–8), as well as *ex vivo* evidence (from autopsy and biopsy samples of cardiac muscle from diabetic patients with congestive heart failure) (9), all indicate a link between insulin resistance (and the associated hyperinsulinemia), and cardiac hypertrophy/heart failure. However the targets of insulin in hypertrophy signaling remain poorly defined.

Recent studies have suggested that the transcription factors myocardin and serum response factor (SRF)[2] may be potential regulators of cardiac gene expression in response to hypertrophy signals (10). SRF, an MCM1, Agamous Deficiens, SRF (MADS)-box transcription factor related to myocyte enhancer factor-2c (MEFc2), interacts with myocardin to bind the DNA consensus sequence CCA/T6GG (CArG box), and is involved in the activation of several cardiac genes, including α-actinin and myosin heavy chain (MHC) (11, 12). Myocardin physically interacts with, and is a target for, ubiquitin-mediated proteolysis via the chaperone-associated ubiquitin (Ub) E3 ligase C terminus of Heat shock Protein 70-interacting protein (CHIP), which functions in protein quality control and plays important roles in cell proliferation and apoptosis (13, 14).

There is a growing consensus that diabetes-induced activation of nuclear factor-κB (NF-κB) contributes to the pro-in-

* This study was supported by Grants R01HL59249 and R01HL69509 from the National Institutes of Health (to Y.-J. G.) and the Italian Istituto Nazionale Ricerche Cardiovascolari (I.N.R.C.) and CARIPLO (to R. M. and R. D. C.).
[1] To whom correspondence should be addressed:Institute of Cardiology, "G. d'Annunzio" University, Chieti, C/o Ospedale SS. Annunziata, Via dei Vestini, 66013 Chieti, Italy. Tel.: 39-0871-41512; Fax: 39-0871-553-461; E-mail: rdecater@unich.it.

[2] The abbreviations used are: SRF, serum response factor; CHIP, C terminus of heat shock protein 70-interacting protein; MHC, myosin heavy chain; PDTC, pyrrolidine dithiocarbamate; CM, cardiac myoblasts; siRNA, small interfering RNA; IR, insulin receptor; SRE, serum response element; MEF, myocyte enhancer factor; MYOCD, myocardin.

flammatory diabetic milieu, including myocardial inflammation, occurring in this condition (15–17). Tumor necrosis factor (TNF)-α, which is found at high levels in patients with insulin resistance, activates NF-κB (18). In turn, NF-κB interacts with other transcription factors, including SRF (19), in inducing inflammation, immune responses, and cellular proliferation (20, 21). In patients with insulin resistance, insulin and TNF-α may synergize in both pro-inflammatory and cardiac hypertrophy signaling. A number of clinical studies have indeed indicated a link between NF-κB activation, cardiac hypertrophy, and cardiovascular disease (22, 23), including diabetic cardiomyopathy (see (24) for a comprehensive review). Despite this body of evidence, the mechanisms and targets by which insulin signals inflammation and hypertrophy remain poorly understood.

Aims of this study were therefore to elucidate the mechanisms of cardiac hypertrophy in insulin resistance, to test whether high insulin levels affect TNF-α-induced activation of NF-κB, and to examine the relationship between myocardin, SRF, and NF-κB in the regulation of the hypertrophy signaling in cardiac myoblasts.

EXPERIMENTAL PROCEDURES

Human Recombinant Insulin—TNF-α, pyrrolidine dithiocarbamate (PDTC), and MTG132 were purchased from Sigma-Aldrich. The Akt/phosphatidyl inositol (PI3)-kinase inhibitor LY294002 was from Calbiochem, La Jolla, CA.

Animal Care—The study population comprised wild-type C57BL/6 (body weight: 22 ± 4 g, $n = 3$ male and $n = 3$ female), and Lepr^{db} (db/db) mice on a C57BL/6 background (homozygotes for a mutation in the leptin receptor gene leading to the loss of a functional leptin receptor) (25) (body weight: 76 ± 5 g, $n = 3$ male and $n = 3$ female), of comparable age (12 months), purchased from The Jackson Laboratories, Bar Harbor, ME. Physiological and biochemical parameters in *db/db* and C57BL/6 mice have been previously reported by us (26). Db/db mice on a C57BL/6J background develop hyperphagia, obesity, and insulin resistance, with severe depletion of the insulin-producing beta-cells of pancreatic islets (25). Their diabetic phenotype, however, is less severe compared with db/db mice on a KsJ background (27). The latter, despite being more severely insulin resistant are less hyperglycemic compared with db/db mice on a C57BL/6J background (27). Db/db mice on C57BL/6J background develop higher plasma fatty acids levels compared with db/db mice on a KsJ background. All animals were specific pathogen-free and kept in a temperature-controlled environment in a ventilated rack with a 12 h:12 h light:dark cycle. Food and water were given *ad libitum*. All procedures were approved by the Institutional Ethics Committee for Animal Research of the University of Texas Health Science Center at Houston). The investigations conformed to the Principles of Laboratory Animal Care formulated by the National Society for Medical Research and the Guide for the Care and Use of Laboratory Animals published by the United States National Institutes of Health.

Cell Culture and Insulin Treatments—Cardiac myoblasts (CMs) were isolated from canine embryonic hearts by collagenase digestion, as previously reported (28). Cells were cultured in Iscove's medium supplemented with 15% embryonic stem cell-qualified fetal bovine serum (FBS) (Stem Cell Technologies, Vancouver, British Columbia, Canada), 2 mM glutamine, 100 IU/ml penicillin, and 0.1 mg/ml streptomycin. At subconfluence, passage 3 CMs were serum-starved for 12 h before being further incubated with insulin (10^{-8} to 10^{-7} mol/liter) for up to 24 h with or without TNF-α (10 ng/ml) or LY294002 (50 μmol/liter). Cell viability after treatments was assessed by evaluating several parameters, including cell morphology and size at phase-contrast microscopy, Trypan Blue exclusion, determination of total proteins.

Cloning of CHIP Expression Plasmids and Transient Transfections—Transfections were performed on subconfluent canine cardiac myoblasts by using Lipofectamine (Invitrogen, Grand Island, NY), according to the manufacturer's specifications. Transfected cells were selected with 400 μg/ml G418 (Sigma-Aldrich) for 15 days. Neomycin-resistant clones were used for further experiments. pcDNA3.1 myc-His expression plasmid (Invitrogen, Catalogue number V855-20) encoding cDNA for human CHIP (GenBank™ accession number NM_005861.2) and pcDNA3.1 myc-His empty vector were a gift from Cam Patterson (among the co-authors of this study) (data not shown). The construct was confirmed by HindIII and XbaI restriction enzyme digest analysis (data not shown). Western analysis was used to analyze protein expression of CHIP in canine cardiac myoblasts by means of anti-CHIP antibody and anti-His_6 antibody (Invitrogen).

Silencing of Myocardin, NF-κB, and CHIP by siRNA—A pool of three different small interfering RNAs (siRNAs) oligonucleotides against CHIP or myocardin or NF-κB, or scrambled negative control siRNAs, were obtained from Ambion. Briefly, 2×10^5 cells/well were plated in 6-well plates in low-serum medium without antibiotics (OptiMem, Invitrogen). Cells were incubated with 6 μl of siRNA transfection reagent containing 15 nmol/liter of one of the following: a mixture of 3 different siRNAs against CHIP, or against myocardin, or against NF-κB or scrambled siRNA (negative control). Transfection medium was added up to a total volume of 800 μl. After 24 h, fresh medium was added, and cells were incubated for an additional 16 h. At the end of incubations, total RNA was harvested for quantitative real-time polymerase chain reaction (qRT-PCR) or protein extracted for Western blotting and electrophoretic mobility shift assay (EMSA), as described below.

RNA Analysis of β-MHC by qRT-PCR—Total RNA was isolated by using a Qiagen RNA isolation kit and used directly for qRT-PCR with the SuperScript™ III Platinum® SYBR® Green One-Step qRT-PCR Kit (Invitrogen) according to the manufacturer's protocol. Primers for qRT-PCR were designed by using the OligoPerfect™ Designer software (Invitrogen). All qRT-PCR reactions were performed in triplicate by using a MyiQ™ single-color RT-PCR detection system (Bio-Rad). A melting curve was generated at the end of every run to ensure product uniformity. Relative expression values were obtained by normalizing CT values of the tested genes in comparison with CT values of the RNA 18 S using the ΔΔCT method.

Immunoprecipitation, in Vitro Ubiquitination, and Immunoblotting—Total or nuclear proteins were extracted as described (29). Proteins were separated under reducing condi-

tions and electroblotted onto polyvinylidene fluoride membranes (Immobilon-P; Millipore, Billerica, MA). After blocking, the membranes were incubated overnight at 4 °C with the following primary antibodies: total or phosphorylated insulin receptor substrate (IRS-1) (Santa Cruz Biotechnology), myocardin (R&D Systems, Minneapolis, MN), MEF2c (Santa Cruz Biotechnology), CHIP (Santa Cruz Biotechnology), ubiquitin (Santa Cruz Biotechnology), lamin-B (Santa Cruz Biotechnology), atrial natriuretic peptide (ANP, Santa Cruz Biotechnology), β-MHC (Santa Cruz Biotechnology), Akt1 isoform and total pAkt (Cell Signaling, Danvers, MA), and β-actin (Sigma). Blots were developed by using a SuperSignal West Pico Chemiluminescent Substrate Kit (Pierce). The intensity of each immunoreactive protein band was measured by densitometry. For immunoprecipitation, the nuclear lysates were mixed with a primary antibody against myocardin (R&D), and immunocomplexes were precipitated with protein-G beads (Sigma). Immunoprecipitates were then eluted, concentrated, and subjected to immunoblotting. For *in vitro* ubiquitination reactions, immunoprecipitates were incubated in 50 μl of control buffer (phosphate-buffered saline) or Ub reaction buffer (30 mM Hepes, pH 7.5, 5 mM $MgCl_2$, 2 mM ATP, 0.2 mM DTT, 10 mM sodium citrate, 10 mM creatine phosphate, and 0.2 μg/ml creatine kinase), 30 nM of E1 enzyme (purchased from Boston Biochem), 0.5 μM of E2 enzyme (Boston Biochem), and 10 μM ubiquitin (Boston Biochem). After incubation at 37 °C for 4 h, reaction products were analyzed by immunoblotting with the indicated antibodies.

Immunofluorescence Microscopy and Cell Size Measurement—Cells grown in eight-well glass chamber slides (Lab-Tek, Pieve D'Alpago, Italy) were fixed with 4% paraformaldehyde, permeabilized, and then blocked in phosphate-buffered saline (PBS) containing 1% bovine serum albumin for 30 min. Cells were incubated in this solution with a primary antibody against α-sarcomeric actinin (Sigma Aldrich) or β-MHC for 1 h at 4 °C. After being incubated and washed in PBS, the slides were incubated with a Texas Red-conjugated anti-rabbit secondary antibody (Invitrogen). Non-immune IgG (Sigma-Aldrich) was used as the isotype control. Slides were washed and mounted with a solution containing 4,6-diamidino-2-phenylindole (VectaShield; Vector Laboratories, Burlingame, CA) and viewed through a fluorescence microscope. The cell surface area of α-sarcomeric actinin-stained cells or unstained cells was measured with the computer-assisted planimetry (N.I.H. Image J) software. The size of adherent cells was assessed by examining 8 different high-power fields (0.09 mm^2/field), randomly located at half-radius distance from the center of the monolayers.

Electrophoretic Mobility Shift Assays (EMSA)—Nuclear proteins were extracted as described (29, 30). Double-stranded serum response element (SRE) consensus oligonucleotides (5′-GGATGTCCATATTAGGACATCT-3′), SRE mutant oligonucleotides (5′-GGATGTCCATATTATTACATCT-3′) (both from Santa Cruz Biotechnology) and NF-κB oligonucleotides (5′-AGT TGA GGG GAC TTT CCC AGG C-3′ and 5′-CCT GGG AAA GTC CCC TCA ACT-3′) (Promega) were labeled with [γ-^{32}P]ATP. Binding reactions containing 10 μg of crude nuclear extract were performed by using an EMSA core system (Promega) according to the manufacturer's protocol. For supershift assays, goat monoclonal anti-myocardin or anti-p65 antibodies (Santa Cruz Biotechnology) were used.

Statistical Analysis—Two-group comparisons were performed with the Student's *t* test for unpaired values. Multiple-group comparisons were performed with the analysis of variance (ANOVA). A p value <0.05 was considered significant.

RESULTS

Myocardin Participates in Mediating Insulin Hypertrophy Signal in Canine Cardiac Myoblasts—Although insulin is known to be able to induce cardiomyocyte hypertrophy (2, 4), and although myocardin is known to be able to mediate hypertrophy signals (31), whether myocardin conveys the hypertrophic signal of insulin is unknown. We therefore explored whether myocardin is necessary for insulin to induce hypertrophy, and analyzed myocardin levels in response to insulin treatment. Treatment of cells with pathophysiologically relevant concentrations of insulin (10^{-8}–10^{-7} mol/liter) increased myocardin levels and activated insulin signaling, as shown by increased levels of phosphorylated IRS-1 (Fig. 1, *panel A*). The Akt-mediated insulin signaling inhibitor LY-294002 attenuated myocardin levels upon insulin treatment. Because MEF2c, a key regulator of early cardiomyogenesis, is known to regulate transcriptional expression of myocardin through its enhancer (32), we also analyzed MEF2c levels in response to insulin treatment. Treatment of cells with insulin (10^{-8}–10^{-7} mol/liter) led to an increase in MEF2c levels (Fig. 1, *panels A* and *B*), which was attenuated by LY-294002 (Fig. 1, *panels A* and *B*). These data suggest that insulin induces myocardin and its activator MEF2c in canine cardiac myoblasts.

To determine if myocardin plays a functional role in insulin-induced hypertrophy, we tested whether the inhibition of myocardin is able to influence hypertrophy. We used siRNA-mediated targeted disruption of myocardin gene expression to specifically block myocardin. Transfection efficiency with myocardin siRNA was >90%. Myocardin siRNA did not affect cell proliferation (data not shown). Treatment with myocardin siRNA, but not a scrambled siRNA sequence, resulted in a substantial (90%) reduction of myocardin protein expression (Fig. 1*D*). Treatment of canine cardiac myoblasts with insulin (10^{-7} mol/liter) resulted in an increase in the hypertrophic marker β-MHC (Fig. 1*C*). Western analysis of ANP did not show any re-expression of this fetal gene in canine cardiac myoblasts at baseline and after insulin treatment (data not shown). Myocardin siRNA attenuated insulin-induced increase in β-MHC expression (Fig. 1*C*). Insulin treatment also led to an increase in cell size of canine cardiac myoblasts, which was inhibited by siRNAs against myocardin (Fig. 1*E*). Thus, myocardin likely participates in conveying the hypertrophy signals of insulin.

Insulin Enhances SRF-SRE Binding—SRF is a nuclear transcription factor that binds to the SRE of DNA sequences located in the promoter of genes critical for cardiovascular myogenesis and cardiac hypertrophy (25, 33, 34). To determine if myocardin, an important co-activator of SRF, can interact with SRF in response to insulin treatment by binding to SREs located in the promoter of such genes, we performed EMSA with nuclear

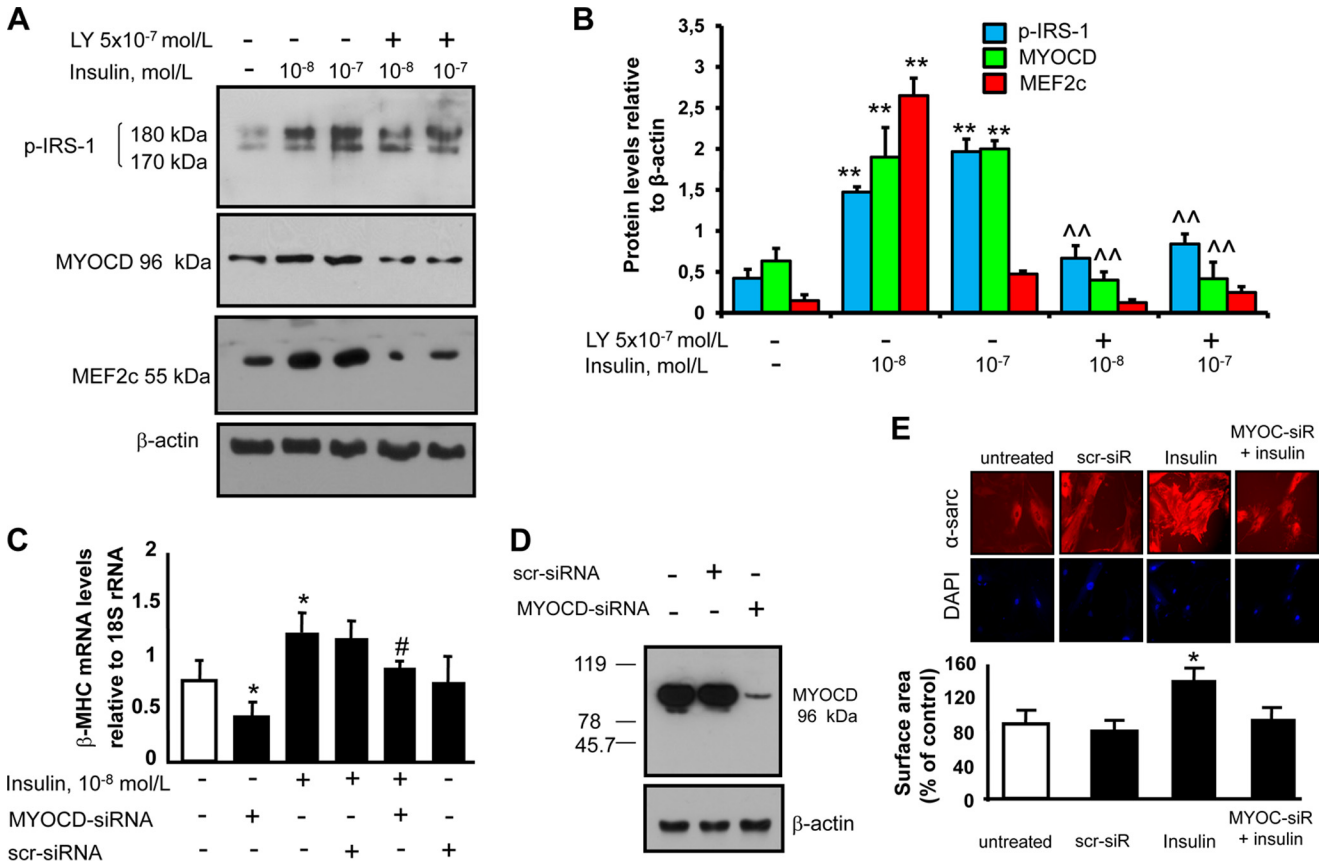

FIGURE 1. **Myocardin induction by insulin and myocardin requirement for insulin-mediated induction of myosin heavy chain-β.** *A* and *B*, myocardin (MYOCD) up-regulation in response to insulin treatment. Canine cardiac myoblasts were starved by growth factor withdrawal and serum reduction (decreased to 2%) for 12 h, followed by stimulation with pathophysiologically relevant concentrations of insulin (10^{-8}-10^{-7} mol/liter) for 24 h with or without the Akt inhibitor LY294002 (5×10^{-7} mol/liter), which was added to the medium 30 min prior to insulin. Following treatments, the expression of myocardin, MEF2c, and p-IRS-1 were detected by immunoblotting. Blots shown are representative of three independent experiments. The results of scanning densitometry ($n =$ 3 independent experiments) are expressed as arbitrary units in *panel B*. Columns and bars represent the mean ± S.D. (**, $p < 0.01$, *versus* untreated cells; ^^, $p <$ 0.01 *versus* insulin-treated cells). *C*, myocardin requirement for insulin-mediated induction of the hypertrophy marker β-MHC. Canine cardiac myoblasts were transfected with a pool of three different siRNAs against myocardin or a scrambled (scr) siRNA (negative control) and treated with insulin (10^{-7} mol/liter) for 6 h. Total RNA was analyzed by real-time quantitative-PCR with primer sets specific for β-MHC. Data (means ± S.D. of three independent experiments) are presented as relative mRNA expression (normalized to RNA 18 S). *, $p < 0.05$ *versus* untreated cells; #, $p < 0.05$ *versus* insulin treated cells. *D*, levels of myocardin in total protein extracts isolated from canine cardiac myoblasts transfected with a pool of three different siRNAs against myocardin or scrambled siRNA (negative control). Blots are representative of three independent experiments. *E*, insulin treatment (10^{-8} mol/liter) led to cell size increase, which was blocked by myocardin-siRNA. Representative photos show cell size of canine cardiac myoblasts. Canine cardiac myoblasts were treated as described for *A–C*. After treatment, cells were permeabilized and fixed for the staining with α-sarcomeric actinin (*α-sarc*). Nuclei were stained with 4′,6-diamidino-2-phenylindole.

extracts from canine cardiac myoblasts treated with insulin (10^{-8}-10^{-7} mol/liter) and incubated with a radiolabeled double-stranded DNA SRE probe ([^{32}P]SRE). SRF-SRE activity, a preliminary requirement for myogenesis, was thus detected (Fig. 2, *panels A* and *B*). In nuclear protein extracts from cells treated with insulin, a strong binding activity was indicated by the appearance of shifted bands. The specificity of the SRF-^{32}P-SRE binding was confirmed with the use of mutant probes or by competition with non-radioactive or mutated probes, which led to the disappearance of shifted bands. Moreover, addition of a specific antibody against myocardin resulted in super-shifted bands (Fig. 2, *panels A* and *B*), indicating that myocardin was present in the protein-SRE probe complexes. Quantitative analysis of the shifted bands confirmed that insulin treatment enhanced SRF binding activity. The Akt inhibitor LY-294002 attenuated the SRF-SRE activity upon insulin treatment. To further confirm that myocardin plays a functional role in insulin-induced SRF-SRE activity, we also tested whether the inhibition of myocardin can influence insulin-induced SRF-SRE activity. Indeed, myocardin siRNA could substantially attenuate the SRF-SRE binding induced by insulin (Fig. 2, *panels C* and *D*). Thus, insulin treatment increases the binding of SRF to the SRE in canine cardiac myoblasts through the activation of myocardin.

Insulin Increases Myocardin Levels and Activity through CHIP—Insulin stimulates the chaperone-associated ubiquitin (Ub) ligase CHIP (35). In turn, CHIP regulates the stability of myocardin protein by interacting with and promoting ubiquitin-mediated degradation of myocardin by the proteasome complex (14). We therefore first tested whether CHIP is regulated by insulin. Insulin treatment of canine cardiac myoblasts led to a significant reduction in CHIP protein levels (Fig. 3, *panels A* and *B*). We then carried out experiments to understand the functional role of CHIP in hypertrophy, and the relationship between CHIP and myocardin in the hypertrophic cascade of insulin. We tested whether CHIP can regulate myocardin activity by SRF-SRE binding upon treatment with insulin, and whether it can influence the expression of the

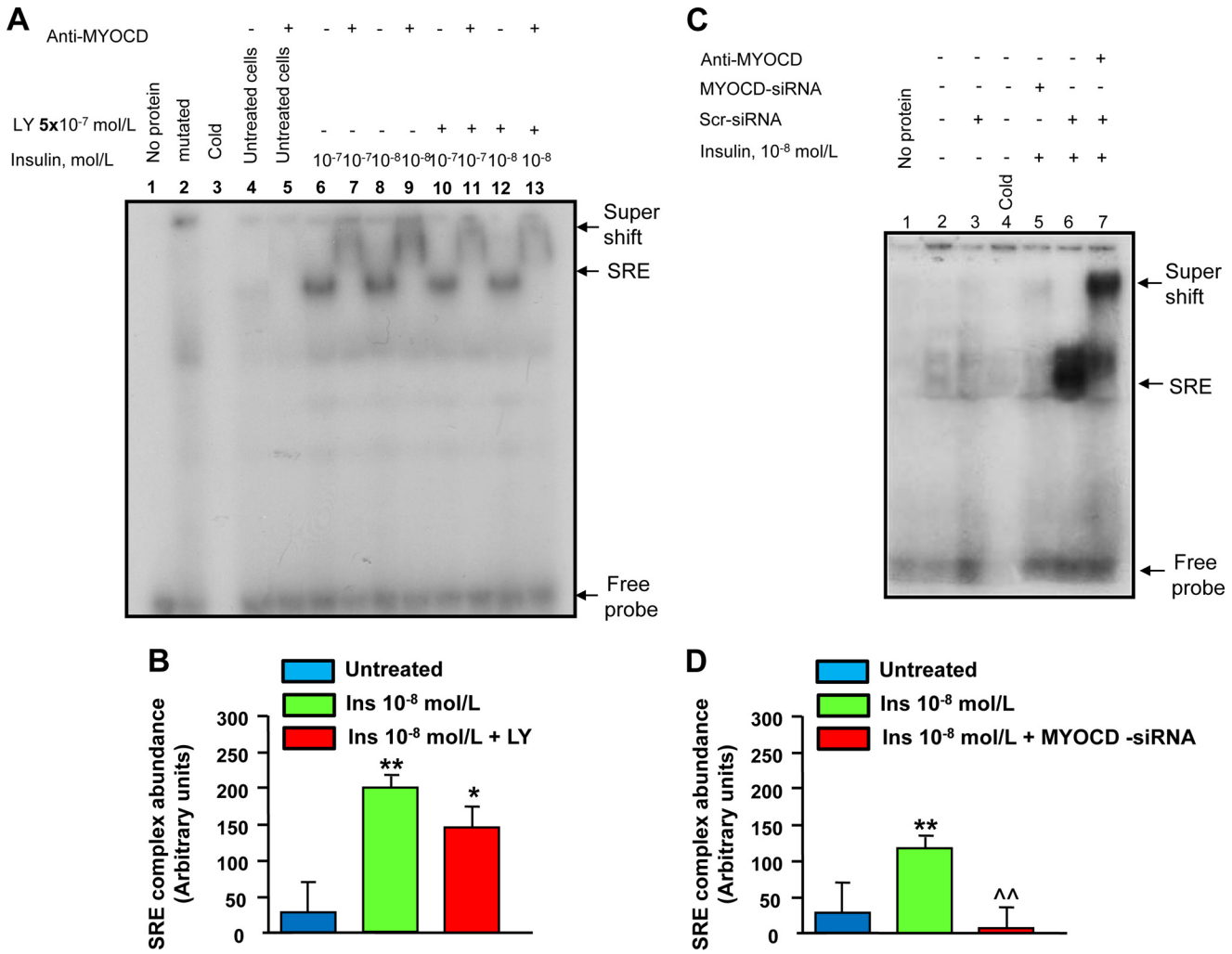

FIGURE 2. **Myocardin requirement for insulin-mediated SRF-SRE binding.** *A*, EMSA assessing the SRF-SRE binding activity in canine cardiac myoblasts in response to insulin. Canine cardiac myoblasts were starved by growth factor withdrawal and serum reduction (decreased to 2%) for 12 h followed by stimulation with pathophysiologically relevant concentrations of insulin (10^{-8}-10^{-7} mol/liter) for 2 h with or without the Akt inhibitor LY294002 (5×10^{-7} mol/liter), which was added to the medium 30 min prior to insulin. Following treatments, nuclear extracts (10 μg) were incubated with or without ^{32}P-end-labeled SRE oligonucleotides. The specificity of the myocardin-SRF-SRE complex formation was determined by competition with either unlabeled oligonucleotide or mutated, labeled SRE oligonucleotides and by the presence of a supershift after the addition of an anti-MYOCD antibody. Here shown is a representative EMSA from three independent experiments are shown. *B*, densitometry of protein-DNA complexes in three different EMSA experiments. **, $p < 0.01$ *versus* untreated cells; *, $p < 0.05$ *versus* insulin treated cells. *C*, canine cardiac myoblasts were transfected with a pool of three different myocardin siRNA oligonucleotides or a scrambled (scr) siRNA (negative control) followed by treatment with insulin (10^{-8}) for 2 h. At the end of the treatment period, nuclear extracts (10 μg) were incubated with or without ^{32}P-end-labeled SRE oligonucleotides. Specificity of the myocardin-SRF-SRE complex formation was determined by the presence of a supershift after the addition of an anti-myocardin antibody. Here shown is a representative EMSA from three independent experiments. *D*, densitometry of protein-DNA complexes in three different EMSA experiments. **, $p < 0.01$ *versus* untreated cells; ^^, $p < 0.01$ *versus* insulin-treated cells.

hypertrophy marker β-MHC. EMSA experiments and Western analyses were performed in canine cardiac myoblasts at baseline and after treatment with insulin (10^{-8}-10^{-7} mol/liter) in the presence or absence of CHIP siRNA and CHIP overexpression.

Overexpression of CHIP in canine cardiac myoblasts was achieved by stable cDNA transfection (data not shown). Transfection efficiency with CHIP siRNA or CHIP-overexpressing plasmid was >90%. Treatment with CHIP siRNA, but not a scrambled siRNA sequence, resulted in a significant (50%) reduction of CHIP protein expression. CHIP siRNA substantially increased the SRF-SRE binding induced by insulin (Fig. 3, *panel D*, *lanes 5* and *6*, and *panel C*), while the proteasome inhibitor MG132 (10 nmol/liter) (Fig. 3, *panel D*, *lanes 4* and *7*, and *panel C*) and CHIP overexpression (Fig. 3, *panel E*, *lanes 11* and *12*, and *panel F*) decreased the SRF-SRE binding induced by insulin. Furthermore, CHIP siRNA, but not a scrambled siRNA sequence, resulted in an increase in the hypertrophy marker β-MHC (Fig. 4, *A* and *C*), while it potentiated the insulin-induced expression of β-MHC (Fig. 4, *A* and *C*). On the contrary, CHIP overexpression (CHIP-TR), but not an empty vector, resulted in a decrease in β-MHC (Fig. 4*B*), while it reverted the insulin-induced expression of β-MHC (Fig. 4*B*). Thus, CHIP is a target of insulin and plays a role as an anti-hypertrophy mediator; and insulin increases myocardin levels and SRF-SRE binding activity in a CHIP-dependent manner.

Finally, we sought to ascertain whether the effect of CHIP on myocardin protein levels occurs through proteasome degrada-

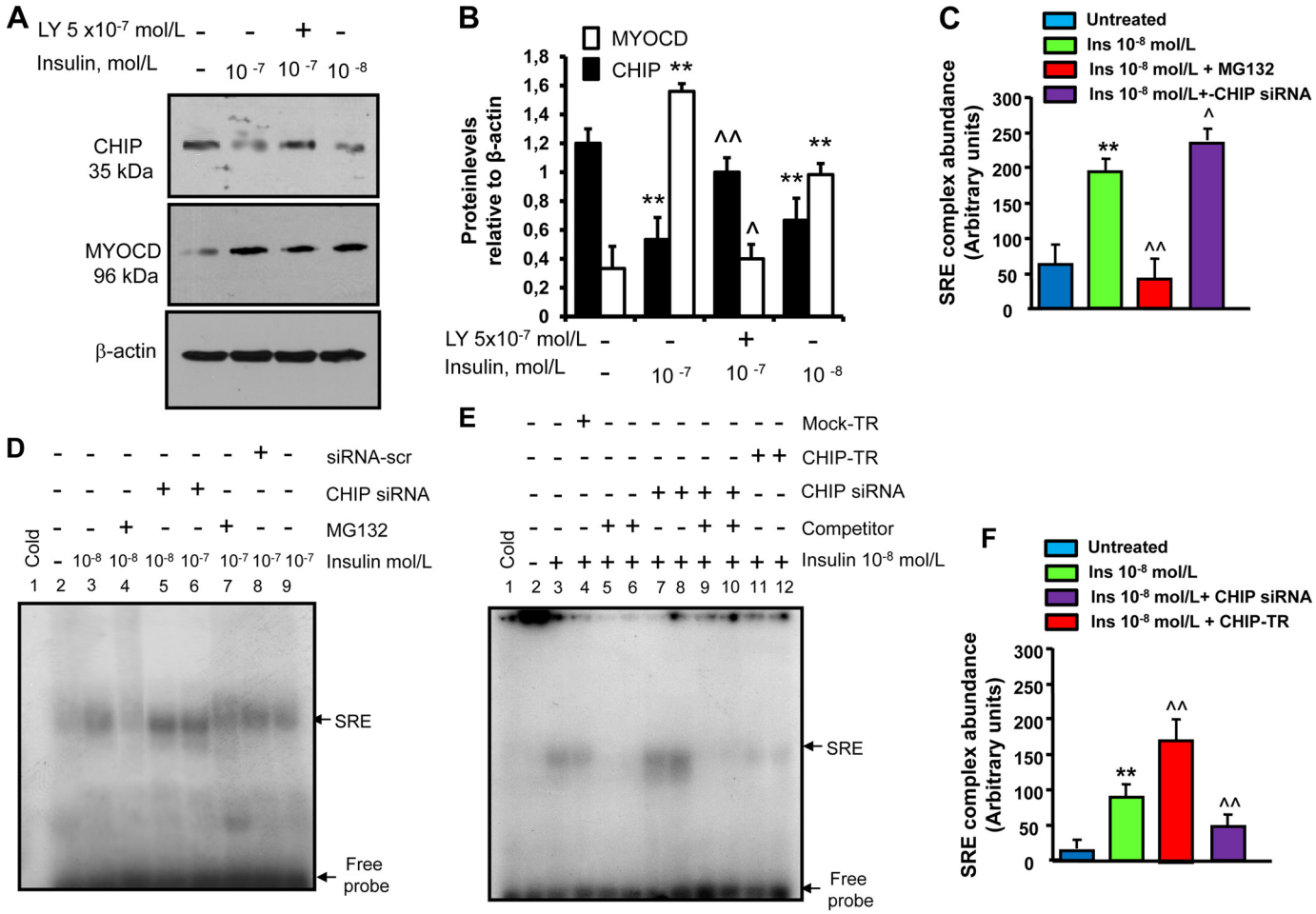

FIGURE 3. **CHIP-dependent insulin induction of myocardin levels and of SRF-SRE binding activity.** *A*, insulin-mediated reduction of chaperone-associated ubiquitin (*Ub*) E3 ligase CHIP. Canine cardiac myoblasts were starved by growth factor withdrawal and serum reduction (decreased to 2%) for 12 h followed by stimulation with pathophysiologically relevant concentrations of insulin (10^{-8}–10^{-7} mol/liter) for 24 h with or without the Akt inhibitor LY294002 (5×10^{-7} mol/liter), which was added to the medium 30 min prior to insulin. Following treatments, CHIP and MYOCD expressions were detected by immunoblotting. Here shown is a blot representative of three independent experiments. *B*, results of scanning densitometry ($n = 3$ independent experiments) expressed as arbitrary optical density units. Columns and bars represent the mean ± S.D. (**, $p < 0.01$ *versus* untreated cells; ^^, $p < 0.01$ *versus* insulin-treated cells; ^, $p < 0.05$ *versus* insulin-treated cells). *C*, densitometry of protein-DNA complexes in three different EMSA experiments represented in *panel D*. **, $p < 0.01$ *versus* untreated cells; ^^, $p < 0.01$ *versus* insulin-treated cells; ^, $p < 0.05$ *versus* insulin treated cells. *D–F*, CHIP-dependent, insulin-mediated increase of SRF-SRE binding activity. *D*, canine cardiac myoblasts were transfected with a pool of three different CHIP siRNA oligonucleotides or a scrambled (scr) siRNA (negative control), and treated with insulin (10^{-8}–10^{-7} mol/liter) for 2 h. A parallel set of cardiac myoblasts was pre-treated with the proteasome inhibitor MG132 (10 μmol/liter) for 6 h prior to the addition of insulin. *E*, canine cardiac myoblasts were mock-transfected (mock-TR, negative control) or transfected with CHIP (CHIP-TR), or transfected with a pool of three different CHIP siRNA oligonucleotides, then treated with 10^{-8} mol/liter insulin for 2 h. After treatments, nuclear extracts (10 μg) were incubated with or without ^{32}P-end-labeled SRE oligonucleotides. Specificity of the SRF-SRE complex formation was determined by showing competition with an unlabeled oligonucleotide. EMSA representatives of three independent experiments are shown. *F*, densitometry of protein-DNA complexes in three different EMSA experiments represented in *panel E*. **, $p < 0.01$ *versus* untreated cells; ^^, $p < 0.01$ *versus* insulin-treated cells.

tion upon insulin treatment (Fig. 4, *panels D* and *E*). We therefore analyzed ubiquitination of myocardin by immunoblotting with an anti-Ub antibody, and looked for high-molecular weight bands. As shown in Fig. 4, panel *E*, ubiquitination of myocardin was substantially decreased with insulin treatment. CHIP siRNA could further decrease myocardin ubiquitination upon insulin treatment (Fig. 4, *panel E*).

TNF-α Potentiates Insulin-induced SRF-SRE Binding Activity and Expression of the Hypertrophy Marker β-MHC—TNF-α is a potent mediator of inflammation and insulin resistance, and is known to synergize with other inflammatory stimuli in increasing intracellular oxidative stress (36). TNF-α activates the redox-sensitive transcription factor NF-κB, which interacts with other families of pro-myogenic transcription factors, including SRF, to induce cardiac hypertrophy (19). In previous work we have shown that insulin synergizes with TNF-α to induce NF-κB activation in endothelial cells (37–40). Here we tested whether insulin could induce NF-κB expression in canine cardiac myoblasts exposed to TNF-α. Insulin treatment indeed led to significant activation of NF-κB and markedly increased TNF-α-induced activation of NF-κB (Fig. 5, *panel A*). The specificity of the NF-κB DNA-protein complex was verified by successful competition with an unlabeled (cold) NF-κB oligonucleotide and by the lack of any binding with a mutated oligonucleotide (not shown). In addition, there was no significant specific binding with the unlabeled (cold) oligonucleotide (Fig. 5, *panel A*, *lane 13*), nor was there any specific binding when either nuclear protein extracts or the oligonucleotide probe were omitted (not shown). Nuclear protein extracts from unstimulated myo-

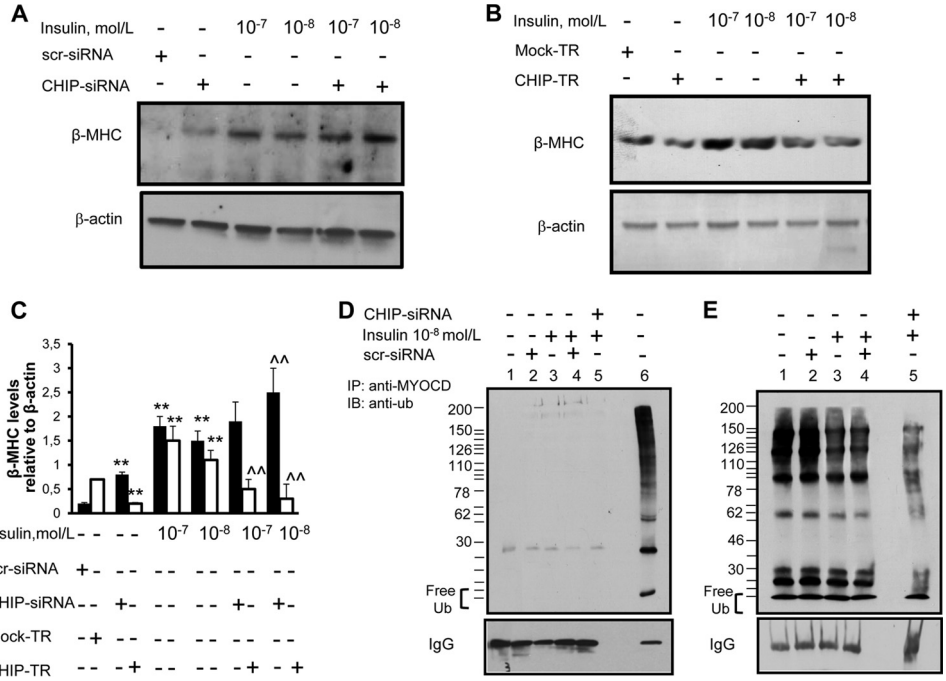

FIGURE 4. **Insulin down-regulation of ubiquitinated CHIP and modulation of myosin heavy chain-β in response to overexpression and silencing of CHIP.** *A*, β-MHC induction in response to CHIP-siRNAs and/or insulin. Canine cardiac myoblasts were transfected with a pool of three different CHIP siRNAs oligonucleotides or a scrambled (scr) siRNA (negative control), and treated with insulin (10^{-8}–10^{-7} mol/liter) for 24 h. *B*, β-MHC repression in response to CHIP overexpression. Canine cardiac myoblasts were either mock-transfected (mock-TR, negative control) or transfected with CHIP (CHIP-TR), then treated with 10^{-8} mol/liter insulin (10^{-8}-10^{-7} mol/liter) for 24 h. Following treatments, the expression of β-MHC was detected by immunoblotting. Blots shown are representative of three independent experiments. *C*, results of scanning densitometry ($n = 3$ independent experiments) expressed as a ratio of β-MHC to β-actin in three different immunoblots represented in *panels A* and *B*. Columns and bars represent the mean ± S.D. (**, $p < 0.01$, *versus* untreated cells; ^^, $p < 0.01$ *versus* insulin-treated cells). *D–E*, insulin-mediated decrease of CHIP ubiquitination. Canine cardiac myoblasts were transfected with a pool of three different CHIP siRNA oligonucleotides or a scrambled siRNA (negative control), and then treated with insulin (10^{-8} mol/liter) for 24 h. Proteins were immunoprecipitated with an anti-myocardin antibody and subjected to ubiquitination reactions (*panel D*, *lane 6* and *panel E*). *Panel D*, *lanes 1–5* shows control experiments with immunoprecipitates incubated in 50 μl of control buffer. Reactions were resolved by sodium dodecyl sulfate-polyacrylamide gel electrophoresis, followed by immunoblotting with anti-Ub antibody (*panels D* and *E*). Here shown is a blot representative of three independent experiments.

blasts also failed to show any specific binding (Fig. 5, *panel A*, *lanes 11–12*).

We next examined the effect of the proteasome inhibitor MG132 (10 nmol/liter), which inhibits NF-κB formation and degradation of its inhibitor I-κB, on insulin-induced NF-κB activation in the presence or absence of TNF-α. In the absence of any cytotoxicity, treatment of canine cardiac myoblasts with MG132 significantly decreased the induction of NF-κB by insulin with or without TNF-α (Fig. 5, *panel A*, *lanes 3–6*). We next carried out experiments to understand the relationship between TNF-α and NF-κB in the insulin-mediated hypertrophy signaling cascade. TNF-α treatment led to a significant increase in SRF-SRE binding and markedly increased insulin-induced activation of SRE, which was further potentiated by CHIP siRNA (Fig. 5, *panel A*, *lanes 1–4*). The antioxidant pyrrolidine dithiocarbamate (PDTC) has been shown in previous work to inhibit NF-κB activation (41). In our study, PDTC substantially reduced the SRF-SRE binding induced by insulin and TNF-α (Fig. 5, *panel B*, *lane 5*). In parallel, TNF-α treatment led to a significant induction of MHC-β expression (Fig. 6, *panels A*, *B*, and *C*) and markedly potentiated the insulin-induced expression of this hypertrophy marker (Fig. 6, *panels A*, *D*, and *E*). NF-κB-directed siRNA significantly decreased the induction of MHC-β expression by insulin with or without TNF-α. These effects were further enhanced by the simultaneous silencing of myocardin and NF-κB, indicating a cooperation between these transcription factors in regulating MHC-β expression (Fig. 6). Taken together, these results demonstrate that both NF-κB and myocardin play a key role in mediating the activation of the pro-myogenic program in canine cardiac myoblasts exposed to insulin and TNF-α.

Hearts of Obese db/db Mice Feature Selective Insulin Resistance Signaling—We then expanded the *in vitro* studies investigating the diabetic mouse heart at 12 months. As expected, *db/db* mice at 12 months of age fed normal chow featured significant body weight gain, with marked elevation of blood lipids, insulin, and glucose. The *db/db* mice were much heavier than non-diabetic C57BL/6J control mice of the same age (26). There was a modestly, but significantly ($p < 0.05$) higher heart weight, as well as heart weight/body weight ratio in db/db compared with C57BL/6J mice. There were also significantly higher blood levels of glucose and insulin, total cholesterol, LDL and VLDL cholesterol, and triglycerides in db/db mice compared with non-diabetic control mice ($p < 0.01$, $p < 0.01$, $p < 0.01$, $p < 0.05$, and $p < 0.01$, respectively, $n = 3$ in each group). Thus, compared with control C57 mice, *db/db* mice developed severe obesity, hyperlipidemia, and hyperglycemia, as also previously reports by us (26).

Here we evaluated protein levels of the insulin receptor (IR) in the hearts of C57BL/6 and *db/db* mice semi-quantitatively by immunoblotting with an anti-IR antibody. Fig. 7*A*, *panel a* shows an immunoblot with a broad brand corresponding to a

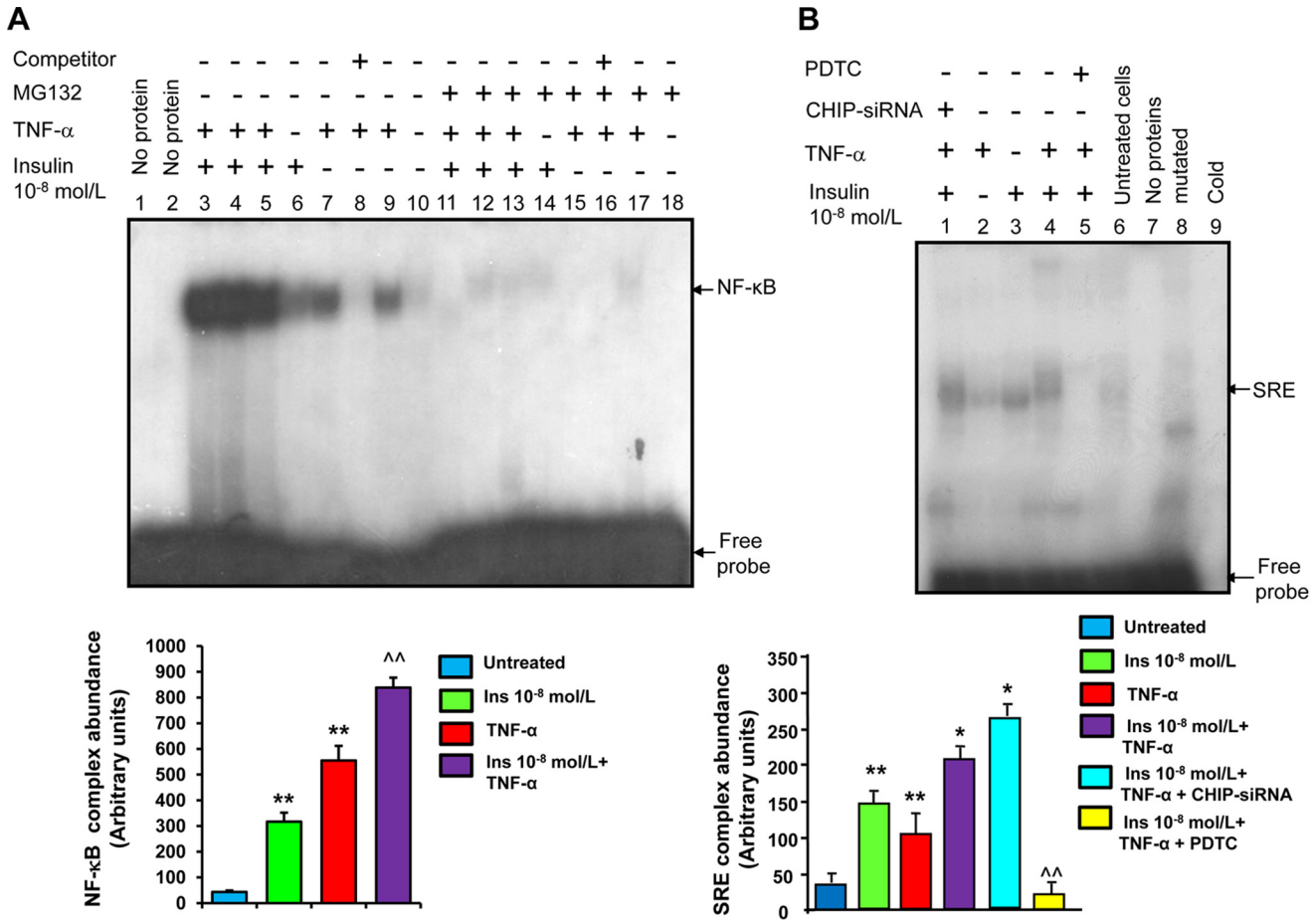

FIGURE 5. **Co-Activation of NF-κB and myocardin/SRF in response to insulin.** *A*, insulin induction of NF-κB in myoblasts exposed to TNF-α. EMSA was performed by mixing the ^{32}P-oligonucleotide containing the NF-κB consensus sequence with nuclear proteins from canine cardiac myoblasts treated with insulin (10^{-8} mol/liter) for 16 h prior to TNF-α stimulation (10 ng/ml, added to cardiac myoblasts during the last 15 min of insulin treatment). A parallel set of cardiac myoblasts was pre-treated with the proteasome inhibitor MG132 (10 nmol/liter) for 6 h prior to insulin addition. The results of an EMSA with nuclear protein extracts from cardiac myoblasts treated with insulin with or without TNF-α (10 ng/ml) or TNF-α alone are shown. Specificity of the SRF-SRE complex formation was determined by competition with an unlabeled oligonucleotide. Results shown here are representative of three independent experiments. *B*, role of NF-κB in mediating the SRF-SRE binding activity in cardiac myoblasts treated with insulin and TNF-α. Canine cardiac myoblasts were transfected with a pool of three different CHIP siRNAs or a scrambled (scr) siRNA (negative control) and treated with insulin (10^{-8} mol/liter) 16 h prior to TNF-α stimulation (10 ng/ml, added to cardiac myoblasts during the last 15 min of insulin treatment). A parallel set of cardiac myoblasts was pre-treated with the NF-κB inhibitor PDTC for 6 h prior to insulin addition. Following treatments, nuclear extracts (10 μg) were incubated with or without ^{32}P-end-labeled SRE oligonucleotides. Specificity of the SRF-SRE complex formation was determined by competition with a cold oligonucleotide and mutated labeled SRE oligonucleotides. Here shown is an EMSA representative of three independent experiments.

protein migrating between 95 and 125 kDa, consistent with the α and β subunits of the IR, indicating no differences between the two groups of mice. Fig. 7*A*, *panel b* shows the phosphoserine proteins in hearts of C57BL/6 and *db/db* mice detected by an antibody against phosphorylated serine 307, revealing a closely spaced doublet with molecular mass between 170 and 185 kDa, consistent with phosphorylation of IRS-1 at serine 307. IRS-1 has numerous phosphorylation sites, consisting of both tyrosine and serine residues, and (depending on the level of hyperphosphorylation) has different electrophoretic mobilities (42, 43). Tyrosine residues are required for the activation of IRS proteins, whereas serine residues are involved in a negative feedback loop, functioning to de-activate IRS proteins (43, 44). While similar tissue levels of total IRS-1 were found in hearts from the two strains of animals studied (not shown), a nearly 2-fold increase of serine 307-phosphorylated IRS-1 was observed in *db/db* compared with C57BL/6 mice ($p < 0.01$, $n = 3$) (Fig. 7*A*, *panel b*). The activity of Akt was evaluated by investigating the phosphorylation of serine 473, which represents the final step of Akt activation together with phosphorylation of threonine 308 (45). As shown in Fig. 7*A*, *panel c*, there was a marked decrease in the expression of phospho-Akt protein in *db/db* compared with C57BL/6 mice. On the contrary, there was an increase of Akt1 isoform expression in the *db/db* mice (Fig. 7*A*, *panel c*). Together, these results indicate that a defect of the PI3-kinase/Akt-dependent insulin signaling in obese *db/db* mice is associated with (and likely depends on) a perturbation in the signaling pathway downstream of the IR, leading to a decrease in the metabolic insulin signaling pathway. In contrast to the activation pattern of PI3K, the pattern of mitogen-activated protein kinase (MAPK) phosphorylation of extracellular signal-regulated kinase (ERK)44 and p38 mirrored that of serine 307 phosphorylation-dependent IRS-1 activation in *db/db* mice. As shown in Fig. 7*A*, *panels d* and *e*, ERK44 phosphorylation was significantly greater (by 6-fold, $p < 0.001$) in *db/db* mice than in control mice. Similar to ERK44, p38

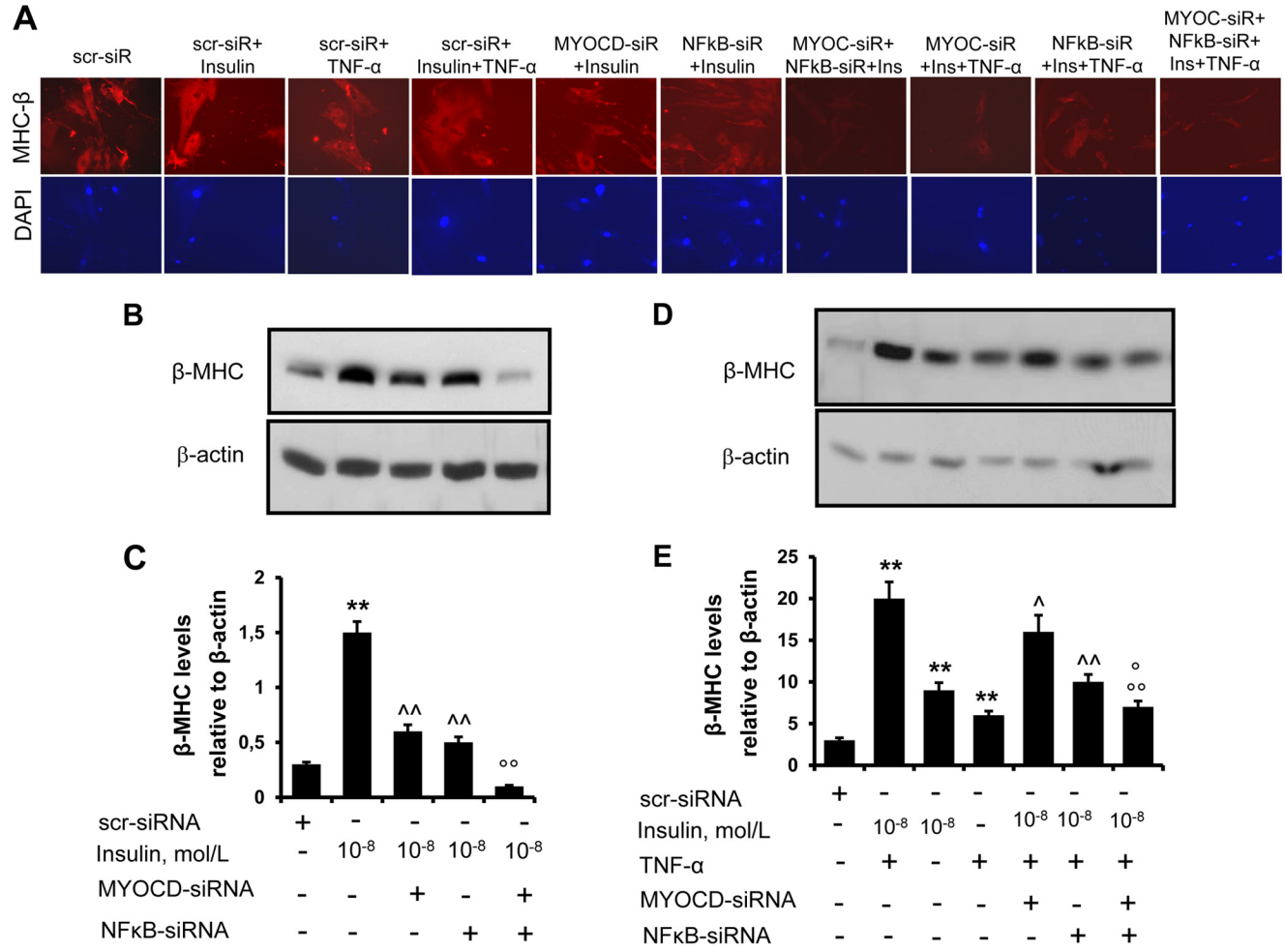

FIGURE 6. **The role of NF-κB and myocardin in mediating myosin heavy chain-β expression in cardiac myoblasts treated with insulin and TNF-α.** *Panel A*, canine cardiac myoblasts were transfected with a pool of three different anti-myocardin siRNAs (MYOCD-siRNA) and/or anti-NF-κB siRNAs or a scrambled (scr) siRNA (negative control), and treated with insulin (10^{-8} mol/liter) with or without TNF-α (10 ng/ml) for 24 h. Following treatments, cells were permeabilized and fixed for the staining with an anti-myosin heavy chain (MHC)-β antibody. Nuclei were stained with 4′,6-diamidino-2-phenylindole. Representative photos show cell size of canine cardiac myoblasts and expression of MHC-β. *Panels B* and *D*, canine cardiac myoblasts were treated as described for A. After treatment, the expression of MHC-β was detected by immunoblotting. Blots shown here are representative of three independent experiments. The results of scanning densitometry ($n = 3$ independent experiments) are expressed as arbitrary units in *panels C* and *D*. Columns and bars represent the mean ± S.D. *Panel C*, **, $p < 0.01$, *versus* untreated cells; ^^, $p < 0.01$ *versus* insulin-treated cells; °°, $p < 0.01$ *versus* insulin + MYOCD-siRNA-treated cells or *versus* insulin + NF-κB -siRNA-treated cells. *Panel E*, **, $p < 0.01$, *versus* untreated cells or *versus* insulin+TNF-α-treated cells; ^, $p < 0.05$ and ^^, $p < 0.01$ *versus* insulin+TNF-α-treated cells; °, $p < 0.05$ and °°, $p < 0.01$ *versus* insulin + MYOCD-siRNA-treated cells or *versus* insulin + NF-κB -siRNA-treated cells.

phosphorylation also increased in *db/db* mice (by 2.5-fold, $p <$ 0.01) compared with wild-type mice (Fig. 7*A*, *panel e*).

Hearts of Obese db/db Mice Show Evidence for Increased Hypertrophy Signaling—Analysis of cardiac tissues in *db/db* mice showed significant up-regulation of myocardin as well as MEF2c at the protein level (Fig. 7*B*, *panels a* and *c*). This increased expression was evident after 4 months and was sustained after 12 months of diabetes, and was associated with decreased expression of CHIP (Fig. 7*B*, *panel d*). Conversely, SRF levels were similar in *db/db* mice compared with age and sex-matched C57BL/6J mice (Fig. 7*B*, *panel b*). In agreement with our previous report (26), diabetic animals also showed increased heart weight (0.4 ± 0.05 g *versus* 0.1 ± 0.03 g, $n = 3$, $p < 0.05$ *db/db* mice *versus* C57 mice) and heart weight to body weight ratio (HW/BW ratio: 0.005 ± 0.05 *versus* 0.004 ± 0.00, $n = 3$, $p < 0.05$ *dbd/db* mice *versus* C57 mice). To determine SRF activity, gel shift assay with ^{32}P end-labeled SRE oligonucleotides was conducted using the nuclear proteins isolated from snap-frozen hearts. As shown in Fig. 8, *panels A* and *B*, SRF binding activities were much stronger in the nuclear extracts from age- and sex-matched hearts of *db/db* mice than those from wild-type controls, indicating their potential for myogenesis. The specificity of the SRF-DNA protein complex formation was verified by competition with cold oligonucleotides. The binding activity with the radioactive oligonucleotide probe was abolished in the absence of protein extracts (Fig. 8, *panel A*, *lane 7*), indicating the dependence of the shifted radioactive bands on nuclear protein factor binding. To determine if myocardin, an important co-activator of SRF, can interact with SRF in the hearts of *db/db* mice, supershift analyses were carried out by adding anti-myocardin antibody (Fig. 8, *panel A*, *lanes 2* and *5*). The antibody to MYOCD super-shifted a portion of the complexes consisting of nuclear protein binding to DNA, indicating that myocardin was present in the protein-SRE probe complexes. Expression and activity of NF-κB were also analyzed in the hearts of *db/db* and C57 mice. In agreement

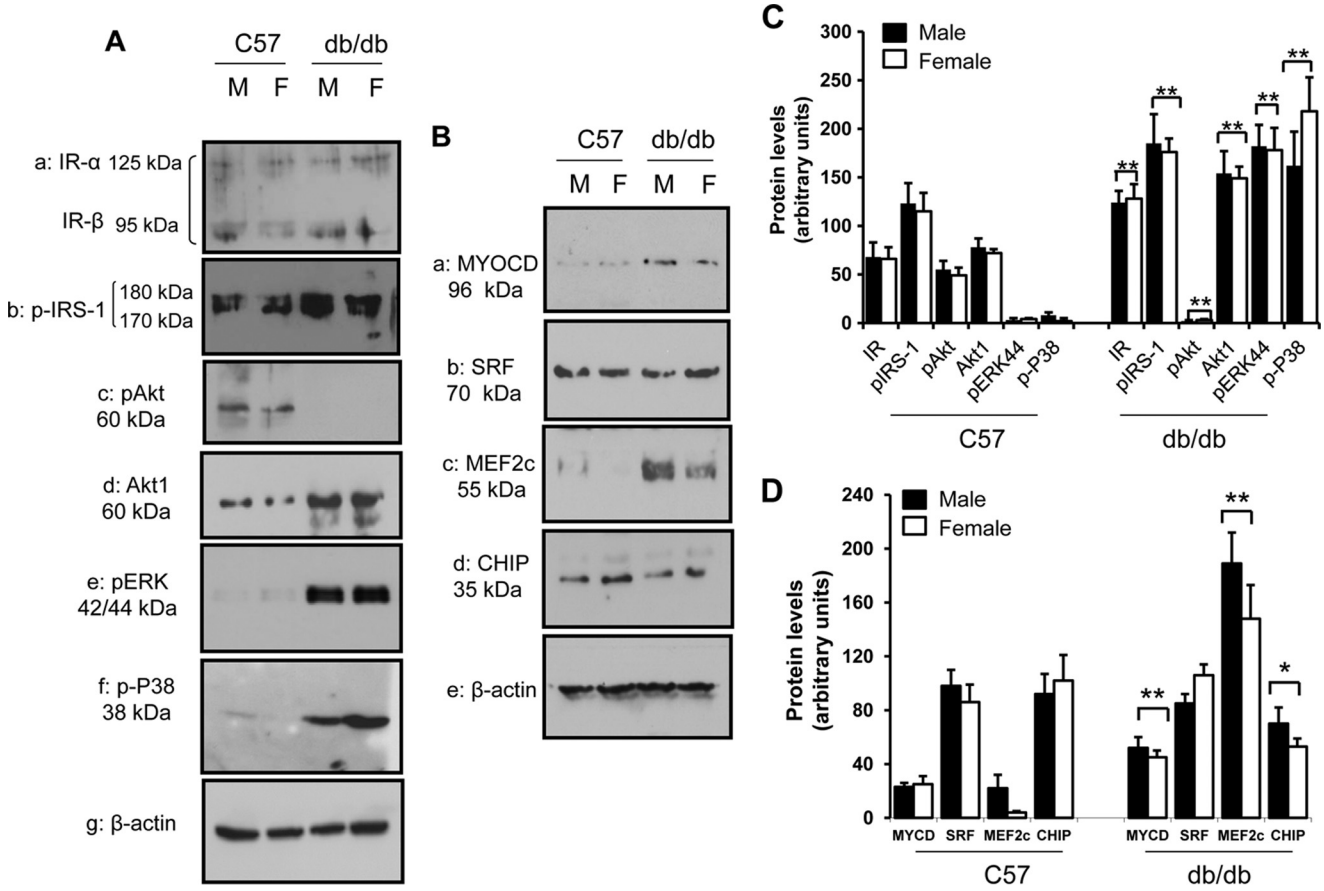

FIGURE 7. **Insulin signaling and Western analysis of cardiomyogenic genes in cardiac tissue of C57BL/6 and *db/db* mice.** *Panel A*, levels of IR subunits α and β, total Akt and the Akt1 isoform, and the phosphorylated isoforms of insulin receptor substrate (IRS)-1, extracellular signal-regulated kinase (ERK)44 and p38 in total protein extracts isolated from male (M) and female (F) *db/db* mice compared with sex- and age-matched C57BL/6 control mice. The blot shown here is representative of three independent experiments. *Panel B*, levels of MYOCD, SRF, MEF 2c, and the CHIP in total protein extracts isolated from male (M) and female (F) *db/db* mice compared with sex- and age-matched C57BL/6 control mice. Blots are representative of three independent experiments. *Panel C*, results of scanning densitometry ($n = 3$ mice per group) of experiments as of *panel A* are expressed as arbitrary units of optical density. Columns and bars represent the mean ± S.D. **, $p < 0.01$, control *versus* non-diabetic control mice. *Panel D*, Results of scanning densitometry ($n = 3$ mice per each group) of experiments as of *panel B* are expressed as arbitrary units of optical density. Columns and bars represent the mean ± S.D. **, $p < 0.01$, control *versus* non-diabetic control mice.

with our previous reports (26), NF-κB binding activities were much stronger in the nuclear extracts from age- and sex-matched hearts of *db/db* mice than those from the wild-type controls (Fig. 8, *panels C* and *D*).

DISCUSSION

A number of clinical studies have indicated a link between insulin resistance/hyperinsulinemia, cardiac hypertrophy and heart failure (6–8). Despite this body of evidence, the downstream targets of insulin in the hypertrophy pathways remain poorly understood. In the present study, we demonstrate that myocardin is a modulator of such insulin-induced hypertrophy.

We used insulin at concentrations that would bind and activate insulin receptors in endothelial cells (between 10^{-9} and 10^{-7} mol/liter) (46). Such concentrations, equivalent to 139–13,900 μU/ml, range from pathophysiological to pharmacological levels of insulinemia. Concentrations of 10^{-9} and 10^{-8} mol/liter are indeed attainable in fasting and post-prandial states in individuals with insulin resistance (47), indicating that our observations are applicable to *in vivo* settings where hyperinsulinemia occurs, with all the caveats of extrapolating from *in vitro* findings.

Myocardin exerts its pro-hypertrophic effect through SRF, which binds to the SRE in the promoter region of genes that are critical for myogenesis (48–50). Previous studies have shown that insulin may initiate a hypertrophy cascade through Akt, which in turn has been demonstrated to control the function of hypertrophy regulators such as nuclear factor of activated T cells (NFAT), GATA-4, and atrogin-1 (51). Our study shows that the Akt inhibitor LY-294002 attenuates myocardin intracellular levels upon insulin treatment. Thus, myocardin can be a downstream target of the insulin/Akt axis in the induction of hypertrophy.

How is myocardin activated in response to insulin signaling? Based on our data, we suggest that at least two mechanisms are involved: 1) myocardin transcripts and protein levels are increased by insulin, which may account for the increase of myocardin-dependent SRF-SRE binding and subsequent activation of the myogenic program; 2) myocardin activity, which is independent of protein expression level, is induced by insulin signaling, most likely through a post-translational change. Pre-

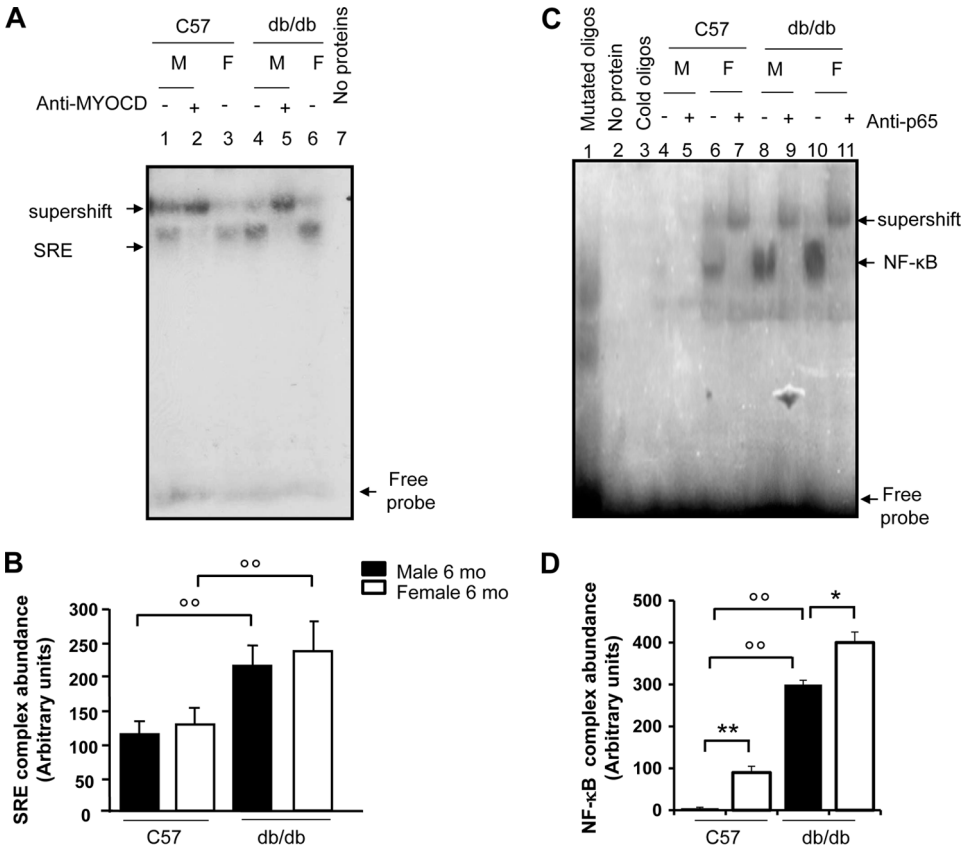

FIGURE 8. **EMSA for myocardin-SRF-SRE and NF-κB binding activities in cardiac tissue of C57BL/6 and *db/db* mice.** *Panel A*, SRF activity was determined by EMSA, performed by mixing a ^{32}P-labeled oligonucleotide encoding for the consensus sequence of serum response element (SRE)-binding promoter with nuclear proteins from male (M) and female (F) *db/db* mouse hearts and sex/age-matched (12-month-old) control hearts (C57BL/6 mice), with $n = 3$ mice per group. Specificity of the myocardin-SRF-SRE complex formation was determined by the omission of nuclear proteins and by the presence of a supershift after the addition of an anti-myocardin antibody. The electrophoretic run with nuclear protein extracts from C57BL/6 control hearts is shown in *lanes 1–3*. The electrophoretic run with nuclear protein extracts from *db/db* mice is shown in *lanes 4–6*. The autoradiogram shown is representative of three separate gel shift experiments for NF-κB. *Lane 7* shows the electrophoretic run by omitting protein extracts. *Panel B*, scanning densitometry ($n = 3$ mice per each group) of the EMSA gels, expressed as arbitrary units of optical density. Columns and bars represent the mean ± S.D. °°, $p < 0.01$, control *versus* diabetic mice. *Panel C*, NF-κB activity was determined by EMSA, performed by mixing a ^{32}P-labeled oligonucleotide encoding for the consensus sequence of the NF-κB-binding promoter with nuclear proteins from the hearts of male (M) and female (F) *db/db* mice and sex- and age-matched C57BL/6 control mice (3 mice per group). Specificity of NF-κB binding activity was evaluated by cold oligonucleotide analysis, the omission of nuclear proteins and by the occurrence of a supershift after the addition of an anti-p65 antibody. The electrophoretic run with nuclear protein extracts from *db/db* mice is shown in *lanes 8–11*. The electrophoretic run with nuclear protein extracts from control hearts (C57BL/6 mice) is shown in lanes 4–7. This autoradiogram is representative three separate gel shift experiments for NF-κB. *Panel D*, scanning densitometry ($n = 3$ mice per each group) of the EMSA gels, expressed as arbitrary units of optical density. Columns and bars represent the mean ± S.D. *, $p < 0.05$ and **, $p < 0.01$, male *versus* female; °°, $p < 0.01$, control *versus* diabetic mice.

vious studies have shown that CHIP promotes the ubiquitination of phosphorylated myocardin and its degradation by the proteasome, thereby inhibiting myocardin-dependent myogenic gene expression (14). In this regard, our results show that insulin down-regulates CHIP, which acts as a repressor of myocardin expression through protein ubiquitination. Furthermore, previous work has shown that MEF2c regulates transcriptional expression of myocardin through its enhancer (32). Our data show that insulin increases levels of MEF2c, which acts as an activator of myocardin expression by enhancing myocardin transcription. Thus, it appears that insulin and its downstream target Akt form an axis with myocardin and its regulators, CHIP and MEF2c, participating in inducing cardiac hypertrophy. Our data are therefore consistent with the hypothesis that myocardin transcription and protein expression are increased by insulin, but do not allow us to determine if post-translational modifications are additionally responsible for insulin-dependent myocardin activation. This point remains to be clarified.

In the *db/db* mouse model also used by us myocardin was up-regulated without the activation of Akt signaling. This discrepancy between the *in vitro* and *in vivo* settings might be due to limitations in having used the *db/db* mice as a model of type 2 diabetes, where the well-known inhibitory effect of hyperglycemia on Akt regulation (52) likely prevails over the effects of hyperinsulinemia. Indeed, unlike other models of type 2 diabetes (*ob/ob* mice, Zucker fatty rats), db/db mice are characterized by an earler and more intense development of hyperglycemia relative to hyperinsulinemia (53). Alternatively, the discrepancy may be due to the specific isoform of Akt chronically regulated *in vivo* by hyperinsulinemia. There is indeed evidence of a divergent regulation of Akt1 and Akt2 in insulin target tissues, where insulin exerts differential effects on these isoforms in a tissue- and species-specific manner (54). Previous studies have shown that chronic hyperinsulinemia may increase myocardial Akt1 activation (55, 56). In the skeletal muscle of obese Zucker rats, Akt2 is reduced, while Akt1 is increased (54).

It is likely that acutely (such as in the *in vitro* model of high insulin concentrations) insulin stimulates growth through the same PI3K/Akt pathway by which it mediates glucose uptake. However, chronically, such as the in *db/db* mice, where insulin resistance and decreased glucose uptake through a down-regulation of PI3K/Akt pathway are present, hyperinsulinemia may stimulate growth through an alternative pathway, by increasing myocardial Akt-1 activation.

Increased circulating levels of pro-inflammatory cytokines, such as interleukin (IL)-6 (57) and tumor necrosis factor (TNF)-α (18), as well as high levels of acute phase reactants (58), have been found in patients with insulin resistance, obesity and type 2 diabetes. Low-grade chronic inflammation may play a role in the pathogenesis of insulin resistance in obesity and type 2 diabetes, as well as in cardiovascular complications of diabetes, including cardiac remodeling and heart failure. We have previously shown that TNF-α synergizes with insulin to induce NF-κB activation and expression of adhesion molecules in endothelial cells (37–40). The present study demonstrates that insulin, alone or in combination with low concentrations of TNF-α, can activate the transcription factor NF-κB in cardiac myoblasts. Previous studies using myoblast cell lines resulted in contradictory results concerning the effect of TNF-α on the activation of the myogenic program (59). The present study has used primary myoblasts, which replicate the properties of cardiomyocytes more closely than myoblast cell lines (60).

In previous studies, cardiac-specific genetic ablation of NF-κB has been shown to attenuate angiotensin II-induced hypertrophy (61), which indicates a key role for NF-κB in the induction of cardiac hypertrophy. Here we show that TNF-α cooperates with insulin in enhancing SRF-SRE binding and inducing the activation of the myogenic program at levels up to 10 ng/ml, a concentration previously shown to evoke signaling events mediated by TNF-α receptor activation in cultured myocytes without inducing necrotic or apoptotic cell death (62). TNF-α stimulation of the myogenic program and hypertrophy appears to involve multiple signaling pathways (63). TNF-α activates NF-κB in cardiomyocytes and myoblasts (22), and in myoblasts in other studies (62, 63). TNF-α stimulation of the myogenic program through SRF signaling is thus likely to involve mediation by NF-κB. We have indeed also shown that the NF-κB inhibitor PDTC, as well as NF-κB silencing attenuate the SRF-SRE binding and the expression of the hypertrophy marker MHC-β upon insulin and TNF-α treatment.

Our experiments were carried out in serum-starved culture conditions (a growth medium supplemented with 2% bovine serum). SRF responds to serum growth factors (64), and the low basal activity of SRF observed in our experiments may reflect the presence of serum growth factors at very low con centrations.

In conclusion, our study reveals that CHIP constitutes an anti-hypertrophy mediator, and can be a target of insulin in the induction of hypertrophy. Insulin cooperates with TNF-α in inducing NF-κB and SRF-SRE activities. Thus, our data shed new light on the understanding of the molecular mechanism through which insulin induces hypertrophy and remodeling during insulin resistance and hyperinsulinemia in type 2 diabetes. Such studies may help designing strategies to prevent diabetic cardiomyopathy (65, 66).

Acknowledgment—We thank Harnath Shelat for help in cell cultures.

REFERENCES

1. Frey, N., and Olson, E. N. (2003) Cardiac hypertrophy: the good, the bad, and the ugly. *Annu. Rev. Physiol.* **65,** 45–79
2. Li, H., Watford, W., Li, C., Parmelee, A., Bryant, M. A., Deng, C., O'Shea, J., and Lee, S. B. (2007) Ewing sarcoma gene EWS is essential for meiosis and B lymphocyte development. *J. Clin. Invest.* **117,** 1314–1323
3. Belke, D. D. (2002) Insulin signaling coordinately regulates cardiac size, metabolism, and contractile protein isoform expression. *J. Clin. Invest.* **109,** 629–639
4. Samuelsson, A. M., Bollano, E., Mobini, R., Larsson, B. M., Omerovic, E., Fu, M., Waagstein, F., and Holmäng, A. (2006) Hyperinsulinemia: effect on cardiac mass/function, angiotensin II receptor expression, and insulin signaling pathways. *Am. J. Physiol. Heart Circ. Physiol.* **291,** H787–H796
5. Shimizu, I., Minamino, T., Toko, H., Okada, S., Ikeda, H., Yasuda, N., Tateno, K., Moriya, J., Yokoyama, M., Nojima, A., Koh, G. Y., Akazawa, H., Shiojima, I., Kahn, C. R., Abel, E. D., and Komuro, I. (2010) Excessive cardiac insulin signaling exacerbates systolic dysfunction induced by pressure overload in rodents. *J. Clin. Invest.* **120,** 1506–1514
6. Paolisso, G., Galzerano, D., Gambardella, A., Varricchio, G., Saccomanno, F., D'Amore, A., Varricchio, M., and D'Onofrio, F. (1995) Left ventricular hypertrophy is associated with a stronger impairment of non-oxidative glucose metabolism in hypertensive patients. *Eur J. Clin. Invest.* **25,** 529–533
7. Hittinger, L., Mirsky, I., Shen, Y. T., Patrick, T. A., Bishop, S. P., and Vatner, S. F. (1995) Hemodynamic mechanisms responsible for reduced subendocardial coronary reserve in dogs with severe left ventricular hypertrophy. *Circulation* **92,** 978–986
8. Rutter, M. K., Parise, H., Benjamin, E. J., Levy, D., Larson, M. G., Meigs, J. B., Nesto, R. W., Wilson, P. W., and Vasan, R. S. (2003) Impact of glucose intolerance and insulin resistance on cardiac structure and function: sex-related differences in the Framingham Heart Study. *Circulation* **107,** 448–454
9. Fonarow, G. C., and Srikanthan, P. (2006) Diabetic cardiomyopathy. *Endocrinol. Metab. Clin. North Am.* **35,** 575–599
10. Zhang, X., Azhar, G., Chai, J., Sheridan, P., Nagano, K., Brown, T., Yang, J., Khrapko, K., Borras, A. M., Lawitts, J., Misra, R. P., and Wei, J. Y. (2001) Cardiomyopathy in transgenic mice with cardiac-specific overexpression of serum response factor. *Am. J. Physiol. Heart Circ. Physiol.* **280,** H1782—H1792
11. Norman, C., Runswick, M., Pollock, R., and Treisman, R. (1988) Isolation and properties of cDNA clones encoding SRF, a transcription factor that binds to the c-fos serum response element. *Cell* **55,** 989–1003
12. Wang, D., Chang, P. S., Wang, Z., Sutherland, L., Richardson, J. A., Small, E., Krieg, P. A., and Olson, E. N. (2001) Activation of cardiac gene expression by myocardin, a transcriptional cofactor for serum response factor. *Cell* **105,** 851–862
13. Ballinger, C. A., Connell, P., Wu, Y., Hu, Z., Thompson, L. J., Yin, L. Y., and Patterson, C. (1999) Identification of CHIP, a novel tetratricopeptide repeat-containing protein that interacts with heat shock proteins and negatively regulates chaperone functions. *Mol. Cell. Biol.* **19,** 4535–4545
14. Xie, P., Fan, Y., Zhang, H., Zhang, Y., She, M., Gu, D., Patterson, C., and Li, H. (2009) CHIP represses myocardin-induced smooth muscle cell differentiation via ubiquitin-mediated proteasomal degradation. *Mol. Cell. Biol.* **29,** 2398–2408
15. Bierhaus, A., Schiefofer, S., Schwaninger, M., Andrassy, M., Humpert, P. M., Chen, J., Hong, M., Luther, T., Henle, T., Kloting, I., Morcos, M., Hofmann, M., Tritschler, H., Weigle, B., Kasper, M., Smith, M., Perry, G., Schmidt, A. M., Stern, D. M., Haring, H. U., Schleicher, E., and Nawroth, P. P. (2001) Diabetes-associated sustained activation of the transcription

factor nuclear factor-κB. *Diabetes Care* **50,** 2792–2808
16. Burke, J. R. (2003) Targeting I κB kinase for the treatment of inflammatory and other disorders. *Curr. Opin. Drug Discov. Devel.* **6,** 720–728
17. Navab, M., Gharavi, N., and Watson, A. D. (2008) Inflammation and metabolic disorders. *Curr. Opin. Clin. Nutr. Metab. Care* **11,** 459–464
18. Mishima, Y., Kuyama, A., Tada, A., Takahashi, K., Ishioka, T., and Kibata, M. (2001) Relationship between serum tumor necrosis factor-α and insulin resistance in obese men with Type 2 diabetes mellitus. *Diabetes Res. Clin. Pract.* **52,** 119–123
19. Franzoso, G., Carlson, L., Brown, K., Daucher, M. B., Bressler, P., and Siebenlist, U. (1996) Activation of the serum response factor by p65/NF-κB. *EMBO J.* **15,** 3403–3412
20. Guttridge, D. C., Mayo, M. W., Madrid, L. V., Wang, C. Y., and Baldwin, A. S., Jr. (2000) NF-κB-induced loss of MyoD messenger RNA: possible role in muscle decay and cachexia. *Science* **289,** 2363–2366
21. Baldwin, A. S., Jr. (2001) Series introduction: the transcription factor NF-κB and human disease. *J. Clin. Invest.* **107,** 3–6
22. Zelarayan, L., Renger, A., Noack, C., Zafiriou, M. P., Gehrke, C., van der Nagel, R., Dietz, R., de Windt, L., and Bergmann, M. W. (2009) NF-κB activation is required for adaptive cardiac hypertrophy. *Cardiovasc. Res.* **84,** 416–424
23. Van der Heiden, K., Cuhlmann, S., Luong le, A., Zakkar, M., and Evans, P. C. (2010) Role of nuclear factor κB in cardiovascular health and disease. *Clin. Sci.* **118,** 593–605
24. Lorenzo, O., Picatoste, B., Ares-Carrasco, S., Ramírez, E., Egido, J., and Tuñón, J. (2011) Potential role of nuclear factor κB in diabetic cardiomyopathy. *Mediators Inflamm.* 2011:652097
25. Chen, C. Y., and Schwartz, R. J. (1996) Recruitment of the tinman homolog Nkx-2.5 by serum response factor activates cardiac α-actin gene transcription. *Mol. Cell. Biol.* **16,** 6372–6384
26. Madonna, R., Wu, H., Shelat, S., and Geng, Y. (2013) CD1d-Associated expression of NF-κB and cardiac dysfunction in diabetic and obese mice. *Int. J. Immunopathol.Pharmacol.* **26,** 59–73
27. Coleman, D. L. (1978) Obese and diabetes: two mutant genes causing diabetes-obesity syndromes in mice. *Diabetologia* **14,** 141–148
28. Madonna, R., Shelat, H., Xue, Q., Willerson, J. T., De Caterina, R., and Geng, Y. J. (2009) Erythropoietin protects myocardin-expressing cardiac stem cells against cytotoxicity of tumor necrosis factor-alpha. *Exp. Cell Res.* **315,** 2921–2928
29. Madonna, R., Di Napoli, P., Massaro, M., Grilli, A., Felaco, M., De Caterina, A., Tang, D., De Caterina, R., and Geng, Y. J. (2005) Simvastatin attenuates expression of cytokine-inducible nitric-oxide synthase in embryonic cardiac myoblasts. *J. Biol. Chem.* **280,** 13503–13511
30. Madonna, R., Willerson, J. T., and Geng, Y. J. (2008) Myocardin a enhances telomerase activities in adipose tissue mesenchymal cells and embryonic stem cells undergoing cardiovascular myogenic differentiation. *Stem Cells* **26,** 202–211
31. Xing, W., Zhang, T. C., Cao, D., Wang, Z., Antos, C. L., Li, S., Wang, Y., Olson, E. N., and Wang, D. Z. (2006) Myocardin induces cardiomyocyte hypertrophy. *Circ. Res.* **98,** 1089–1097
32. Creemers, E. E., Sutherland, L. B., McAnally, J., Richardson, J. A., and Olson, E. N. (2006) Myocardin is a direct transcriptional target of Mef2, Tead and Foxo proteins during cardiovascular development. *Development* **133,** 4245–4256
33. Belaguli, N. S., Schildmeyer, L. A., and Schwartz, R. J. (1997) Organization and myogenic restricted expression of the murine serum response factor gene. A role for autoregulation. *J. Biol. Chem.* **272,** 18222–18231
34. Sepulveda, J. L., Belaguli, N., Nigam, V., Chen, C. Y., Nemer, M., and Schwartz, R. J. (1998) GATA-4 and Nkx-2.5 coactivate Nkx-2 DNA binding targets: role for regulating early cardiac gene expression. *Mol. Cell. Biol.* **18,** 3405–3415
35. Belova, L., Sharma, S., Brickley, D. R., Nicolarsen, J. R., Patterson, C., and Conzen, S. D. (2006) Ubiquitin-proteasome degradation of serum- and glucocorticoid-regulated kinase-1 (SGK-1) is mediated by the chaperone-dependent E3 ligase CHIP. *Biochem. J.* **400,** 235–244
36. Jersmann, H. P., Hii, C. S., Ferrante, J. V., and Ferrante, A. (2001) Bacterial lipopolysaccharide and tumor necrosis factor α synergistically increase expression of human endothelial adhesion molecules through activation of NF-κB and p38 mitogen-activated protein kinase signaling pathways. *Infect Immun.* **69,** 1273–1279
37. Madonna, R., Massaro, M., Pandolfi, A., Consoli, A., and De Caterina, R. (2007) The prominent role of p38 mitogen-activated protein kinase in insulin-mediated enhancement of VCAM-1 expression in endothelial cells. *Int. J. Immunopathol. Pharmacol.* **20,** 539–555
38. Madonna, R., Massaro, M., and De Caterina, R. (2008) Insulin potentiates cytokine-induced VCAM-1 expression in human endothelial cells. *Biochim. Biophys. Acta* **1782,** 511–516
39. Madonna, R., and De Caterina, R. (2009) Prolonged exposure to high insulin impairs the endothelial PI3-kinase/Akt/nitric oxide signaling. *Thromb. Haemost.* **101,** 345–350
40. Madonna, R., Salerni, S., Schiavone, D., Glatz, J. F., Geng, Y. J., and De Caterina, R. (2011) Omega-3 fatty acids attenuate constitutive and insulin-induced CD36 expression through a suppression of PPARαγ activity in microvascular endothelial cells. *Thromb. Haemost.* **106,** 500–510
41. Kim, C. H., Kim, J. H., Lee, J., Hsu, C. Y., and Ahn, Y. S. (2003) Thiol antioxidant reversal of pyrrolidine dithiocarbamate-induced reciprocal regulation of AP-1 and NF-κB. *Biol. Chem.* **384,** 143–150
42. Greene, M. W., and Garofalo, R. S. (2002) Positive and negative regulatory role of insulin receptor substrate 1 and 2 (IRS-1 and IRS-2) serine/threonine phosphorylation. *Biochemistry* **41,** 7082–7091
43. Herschkovitz, A., Liu, Y. F., Ilan, E., Ronen, D., Boura-Halfon, S., and Zick, Y. (2007) Common inhibitory serine sites phosphorylated by IRS-1 kinases, triggered by insulin and inducers of insulin resistance. *J. Biol. Chem.* **282,** 18018–18027
44. Tremblay, F., Brûlé, S., Hee Um, S., Li, Y., Masuda, K., Roden, M., Sun, X. J., Krebs, M., Polakiewicz, R. D., Thomas, G., and Marette, A. (2007) Identification of IRS-1 Ser-1101 as a target of S6K1 in nutrient- and obesity-induced insulin resistance. *Proc. Natl. Acad. Sci. U.S.A.* **104,** 14056–14061
45. Datta, S. R., Brunet, A., and Greenberg, M. E. (1999) Cellular survival: a play in three Akts. *Genes Dev.* **13,** 2905–2927
46. Lee, J., and Pilch, P. F. (1994) The insulin receptor: structure, function, and signaling. *Am. J. Physiol.* **266,** C319–C334
47. Saad, M. F., Knowler, W. C., Pettitt, D. J., Nelson, R. G., Mott, D. M., and Bennett, P. H. (1989) Sequential changes in serum insulin concentration during development of non-insulin-dependent diabetes. *Lancet* **1,** 1356–1359
48. Wang, Z., Wang, D. Z., Hockemeyer, D., McAnally, J., Nordheim, A., and Olson, E. N. (2004) Myocardin and ternary complex factors compete for SRF to control smooth muscle gene expression. *Nature* **428,** 185-189
49. Madonna, R., Wu, D., Wassler, M., De Caterina, R., Willerson, J. T., Geng, Y.J. (2013) Myocardin-A enhances expression of promyogenic genes without depressing telomerase activity in adipose tissue-derived mesenchymal stem cells. *Int. J. Cardiol.* **167,** 2912–2921
50. Madonna, R., Taylor, D. A., Geng, Y. J., De Caterina, R., Shelat, H., Perin, E. C., Willerson, J. T. (2013) Transplantation of mesenchymal cells rejuvenated by the overexpression of telomerase and myocardin promotes revascularization and tissue repair in a murine model of hindlimb ischemia. *Circ. Res.* **113,** 902–914
51. Shiojima, I., and Walsh, K. (2006) Regulation of cardiac growth and coronary angiogenesis by the Akt/PKB signaling pathway. *Genes Dev.* **20,** 3347–3365
52. Park, C. W., Kim, H. W., Lim, J. H., Yoo, K. D., Chung, S., Shin, S. J., Chung, H. W., Lee, S. J., Chae, C. B., Kim, Y. S., and Chang, Y. S. (2009) Vascular endothelial growth factor inhibition by dRK6 causes endothelial apoptosis, fibrosis, and inflammation in the heart via the Akt/eNOS axis in db/db mice. *Diabetes* **58,** 2666–2676
53. Poornima, I. G., Parikh, P., and Shannon, R. P. (2006) Diabetic cardiomyopathy: the search for a unifying hypothesis. *Circ. Res.* **98,** 596–605
54. Kim, Y. B., Peroni, O. D., Franke, T. F., and Kahn, B. B. (2000) Divergent regulation of Akt1 and Akt2 isoforms in insulin target tissues of obese Zucker rats. *Diabetes* **49,** 847–856
55. Morisco, C., Condorelli, G., Trimarco, V., Bellis, A., Marrone, C., Condorelli, G., Sadoshima, J., and Trimarco, B. (2005) Akt mediates the cross-talk between β-adrenergic and insulin receptors in neonatal cardiomyocytes. *Circ. Res.* **96,** 180–188

56. O'Neill, B. T., and Abel, E. D. (2005) Akt1 in the cardiovascular system: friend or foe?. *J. Clin. Invest.* **115,** 2059–2064
57. Fernandez-Real, J. M., Vayreda, M., Richart, C., Gutierrez, C., Broch, M., Vendrell, J., and Ricart, W. (2001) Circulating interleukin 6 levels, blood pressure, and insulin sensitivity in apparently healthy men and women. *J. Clin. Endocrinol. Metab.* **86,** 1154–1159
58. McMillan, D. E. (1989) Increased levels of acute-phase serum proteins in diabetes. *Metabolism* **38,** 1042–1046
59. Langen, R. C., Schols, A. M., Kelders, M. C., Wouters, E. F., and Janssen-Heininger, Y. M. (2001) Inflammatory cytokines inhibit myogenic differentiation through activation of nuclear factor-κB. *FASEB J.* **15,** 1169–1180
60. Blau, H. M., Pavlath, G. K., Hardeman, E. C., Chiu, C. P., Silberstein, L., Webster, S. G., Miller, S. C., and Webster, C. (1985) Plasticity of the differentiated state. *Science* **230,** 758–766
61. Esposito, G., Rapacciuolo, A., Naga Prasad, S. V., Takaoka, H., Thomas, S. A., Koch, W. J., and Rockman, H. A. (2002) Genetic alterations that inhibit in vivo pressure-overload hypertrophy prevent cardiac dysfunction despite increased wall stress. *Circulation* **105,** 85–92
62. Li, Y. P., and Schwartz, R. J. (2001) TNF-α regulates early differentiation of C2C12 myoblasts in an autocrine fashion. *FASEB J.* **15,** 1413–1415
63. Moylan, J. S., Smith, J. D., Chambers, M. A., McLoughlin, T. J., and Reid, M. B. (2008) TNF induction of atrogin-1/MAFbx mRNA depends on Foxo4 expression but not AKT-Foxo1/3 signaling. *Am. J. Physiol. Cell Physiol.* **295,** C986–C993
64. Treisman, R. (1986) Identification of a protein-binding site that mediates transcriptional response of the c-fos gene to serum factors. *Cell* **46,** 567–574
65. Karnik, A. A., Fields, A. V., and Shannon, R. P. (2007) Diabetic cardiomyopathy. *Curr. Hypertens Rep.* **9,** 467–473
66. Maisch, B., Alter, P., and Pankuweit, S. (2011) Diabetic cardiomyopathy–fact or fiction?. *Herz* **36,** 102–115

Co-Activation of Nuclear Factor-κB and Myocardin/Serum Response Factor Conveys the Hypertrophy Signal of High Insulin Levels in Cardiac Myoblasts

Rosalinda Madonna, Yong-Jian Geng, Roberto Bolli, Gregg Rokosh, Peter Ferdinandy, Cam Patterson and Raffaele De Caterina

J. Biol. Chem. 2014, 289:19585-19598.
doi: 10.1074/jbc.M113.540559 originally published online May 22, 2014
